Import of adenovirus DNA involves the nuclear pore complex receptor CAN/Nup214 and histone H1

Lloyd C. Trotman*, Nicole Mosberger*, Maarten Fornerod†, Robert P. Stidwill* & Urs F. Greber*‡

**University of Zürich, Institute of Zoology, Winterthurerstrasse 190, CH-8057 Zürich, Switzerland*
†Netherlands Cancer Institute, Plesmanlaan 121, 1066 CX Amsterdam, The Netherlands
‡e-mail: ufgreber@zool.unizh.ch

Adenovirus type 2 (Ad2) imports its DNA genome through the nuclear pore complex (NPC) of cells in interphase for viral production. Here we identify the NPC-filament protein CAN/Nup214 as a docking site for incoming Ad2 capsids. Binding to CAN is independent of cytosolic factors. Capsids disassemble at NPCs to free their DNA for import. This process requires binding of nuclear histone H1 to the stably docked capsids and involves H1-import factors, restricting this irreversible process to the proximity of the nucleus. Our results provide a molecular mechanism for disassembly of Ad2 and reveal an unexpected function of histone H1 in virus-mediated DNA import.

Many viruses subvert host cells by importing their DNA genomes into the host cell nucleus. This feature is essential for the ability of, for example, the lentivirus human immunodeficiency virus (HIV-1) to infect nondividing cells[1]. But the underlying mechanisms of viral gene delivery are still poorly understood.

Adenovirus type 2 (Ad2) transports its DNA genome in a protective 90-nm protein capsid from the cell surface to the NPC. The compacted DNA is subsequently released from the capsid and enters the nucleus alone[2,3]. A hallmark feature of Ad2 infection is an exceptionally fast and efficient transfer of DNA into the nucleus of the host cell. Incoming Ad2 particles receive cues that trigger destabilization already at the cell surface[4,5]. It is only at the NPC that Ad2 receives the cue for final capsid disruption[3], which we refer to as Ad (or capsid) disassembly.

The NPC is built of a diverse set of nucleoporins and associated nuclear and cytoplasmic filaments around a central channel

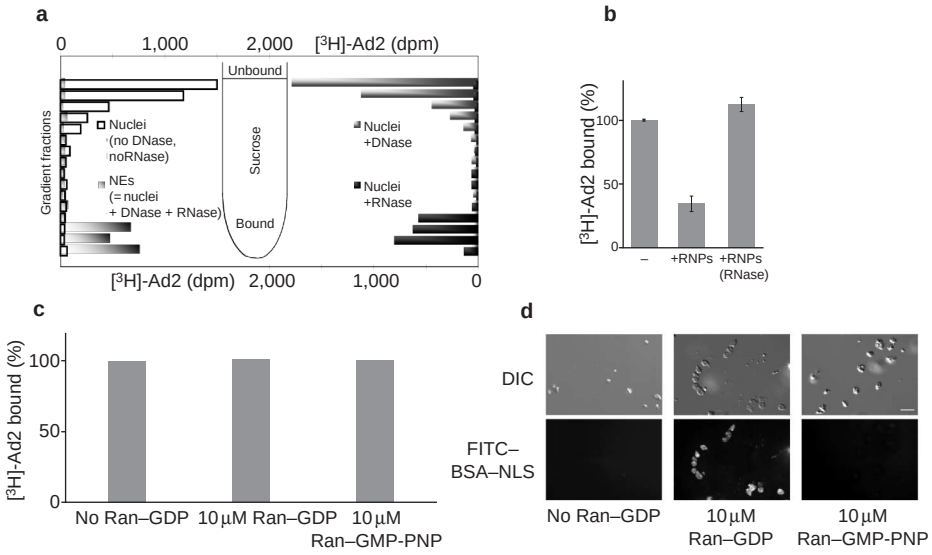

Figure 1 **Ad2 binding to nuclear envelopes is cytosol- and Ran-independent.** **a**, Ad2 binds NEs and RNase-treated nuclei. Rat liver nuclei or NEs were digested with nucleases as indicated, purified, incubated with [3H]-Ad2 at 4 °C for 45 min and centrifuged through a sucrose gradient to separate bound from unbound virus. [3H]-d.p.m. were measured by scintillation counting. **b**, RNPs compete for binding of [3H]-Ad2 to NEs. [3H]-Ad2 was incubated with NEs alone or in the presence of RNPs from a reticulocyte lysate treated or not treated with RNase. Means and standard deviations of duplicates are shown. **c**, Ad2 binding to NEs is not affected by Ran. NEs were preincubated with Ran–GDP or with Ran loaded with GMP-PNP (a nonhydrolysable GTP analogue) and [3H]-Ad2 binding to NEs was determined as described above. **d**, Ran–GDP stimulates association of FITC–BSA–NLS with NEs. NEs were incubated with Ran–GDP or Ran–GMP-PNP as indicated in **c** followed by incubation with 0.5 mg ml^{-1} FITC–BSA–NLS for 1 h and analysis by fluorescence microscopy. Note that FITC–BSA–NLS only binds to Ran–GDP-treated NEs and that the effect of Ran–GDP is effectively abolished by preloading it with GMP-PNP. [3H]-Ad2 binding to these NEs is both independent of Ran–GDP and Ran–GMP-PNP (see **c**). DIC, differential-interference contrast. Scale bar, 20 μm

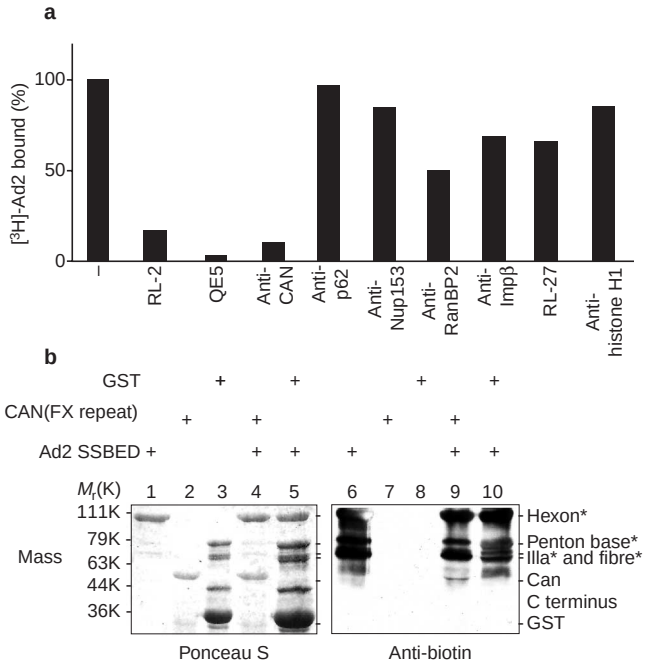

Figure 2 **The NPC protein CAN/Nup214 is a docking site for Ad2.** **a**, Antibody effects on the binding of Ad2 to NEs. NEs were preincubated with the indicated antibodies for 1 h at 4 °C and subjected to [^{3}H]-Ad2 binding assays as described in Fig. 1a. All antibodies that recognized CAN/Nup214 interfered with virus binding to NEs. Note that anti-histone H1 antibodies had no effect. **b**, Ad2–SSBED crosslinks CAN/Nup214. Ad2–SSBED was incubated with bacterially expressed, purified C terminus of CAN/Nup214, or with an *Escherichia coli* extract containing GST and incubated at room temperature for 45 min. Samples were crosslinked by ultraviolet illumination, reduced and analysed for biotin transfer by anti-biotin western blotting (lanes 6–10). Total protein was revealed by Ponceau S staining (lanes 1–5). Asterisks indicate adenoviral proteins.

structure[6–8]. Proteins targeted to the nucleus typically contain sequences recognized by transport receptors of the importin/karyopherin family. This recognition occurs preferentially in the cytosol and is controlled by the GTPase Ran. Low cytoplasmic levels of Ran–GTP permit formation of import complexes, whereas high concentrations of nuclear Ran–GTP favour disruption[9]. The cargo–receptor complex docks and translocates through the pore using specific NPC interactions and is dissociated on the nuclear side after binding Ran–GTP[7,10]. Although this model aptly describes the current knowledge of protein import, its validity for import of large cargo such as cellular ribonucleoproteins (RNPs) or viruses remains to be tested.

Here we delineate a molecular mechanism for Ad2-mediated delivery of DNA into the nucleus (Ad2 import). We find that Ad2 particles bind to the NPC *in vitro* via the fibril protein CAN/Nup214, independently of additional cytosolic factors and independently of Ran–GTP. We also observe *in vivo* that the two immediate downstream events of NPC binding, Ad disassembly and DNA import, are strictly dependent on this binding event. Surprisingly, we find that nuclear histone H1 serves to disassemble Ad2 by binding to NPC-docked particles, and that this disassembly is linked to recruitment of H1-nuclear-import factors.

Results

Ad2 binds the NPC filament protein CAN/Nup214. We first analysed the requirements of binding of Ad2 to NPCs *in vitro* by incubating [^{3}H]-thymidine-labelled virus with isolated rat liver nuclei at 4 °C and separated bound from unbound virus by pelleting the nuclei through sucrose. Ad2 had no affinity for rat liver nuclei but bound quantitatively to so-called nuclear envelopes (NEs; Fig. 1a), that is, nuclei treated with DNase and RNase (see ref. 11, for example). Although RNase treatment alone was sufficient to make nuclei competent for quantitative binding of Ad2 (Fig. 1a), we performed the following binding experiments with NEs, because they have a lower tendency to form aggregates. Virus binding to NEs was independent of cytosol, consistent with earlier results[12], and we found that rabbit reticulocyte lysate quantitatively inhibited binding of Ad2, even though it fully supported nuclear import of FITC–BSA–NLS (fluorescein isothiocyanate–bovine serum albumin–nuclear localization signal) in digitonin-permeabilized HeLa cells (data not shown). We enriched the inhibitory activity by gel filtration and recovered a fraction containing RNA and a discrete set of proteins from the flow through (data not shown). The inhibitory activity was abrogated by treatment with RNase (Fig. 1b), suggesting that it was an RNP. Notably, Ad2-binding to NEs was not affected by an excess of Ran loaded with GMP-PNP, a nonhydrolysable analogue of GTP, or with Ran–GDP (Fig. 1c). Ran–GDP, but not Ran–GMP-PNP, rendered NEs competent to bind FITC–BSA–NLS, indicating functionality of our recombinant Ran (Fig. 1d). Competition experiments of Ad2–NE binding to viral capsid proteins purified from infected cells showed that the protein hexon had the strongest effect (77% reduction), penton base had a moderate (37%) and fibre had no effect.

Next, we examined whether *in vitro* Ad2-binding was specific for NPCs. NEs were preincubated with a panel of antibodies against nucleoporins before adding [^{3}H]-Ad2. The monospecific antibodies RL-2 and QE5, which recognize multiple nucleoporins[11,13], had the strongest inhibitory effects (Fig. 2a), similar to RL-1 (data not shown). Three nucleoporins are commonly recognised by RL-1, RL-2 and QE5: the cytoplasmic filament protein CAN/Nup214, the central protein p62 and the nuclear basket component Nup153 (ref. 6). Monospecific antibodies against these proteins showed that only an antibody to the carboxy-terminal domain of CAN/Nup214 (ref. 14) almost quantitatively prevented Ad2-binding to NEs (Fig. 2a). Antibodies against p62 and Nup153 had no significant effects, similar to the effects of antibodies against importin β (Impβ) (3E9; ref. 15) or RanBP2 (also named Nup358; ref. 16), the docking site of Impβ, or against the lumenal domain of gp210 (RL27; ref. 17). When microinjected into human A549 cells, the anti-p62, anti-Nup153 and anti-RanBP2 antibodies, but not the anti-gp210 lumenal domain antibody, resulted in nuclear-rim staining and inhibited nuclear import of co-injected FITC–BSA–NLS (Supplementary Information Fig. S1), consistent with results published previously[18]. Together, these data demonstrate that binding of Ad2 to NEs requires the NPC-filament protein CAN/Nup214 and is RNP-sensitive, but independent of cytosolic factors and the Ran system.

To test whether Ad2 bound directly to CAN/Nup214, isolated Ad2 was modified with the photoactivatable crosslinking agent Sulfo-SBED (SSBED). SSBED is designed to transfer a biotin moiety onto crosslinked proteins, and can be cleaved by a reducing agent. The predominant crosslinking products were the viral proteins hexon, penton base, fibre and IIIa as detected by western blotting using anti-biotin antibodies and the total protein stain Ponceau S (Fig. 2b, lanes 1 and 6). When SSBED–Ad2 was incubated with the purified, bacterially expressed C-terminal fragment of CAN/Nup214 (which has a relative molecular mass of 50,000 (M_r 50K)), crosslinked using ultraviolet light and reduced with β-mercaptoethanol, the CAN/Nup214 fragment became tagged with biotin (lanes 4 and 9). This biotinylation required Ad2–SSBED (lanes 2 and 7). A bacterial extract predominantly containing glutathione-S-transferase (GST) was not biotin labelled after incubation with Ad2–SSBED (lanes 5 and 10). These results demonstrate that Ad2 can directly bind to the C terminus of CAN/Nup214 *in vitro* and that import factors are not required for this interaction.

CAN/Nup214 is required for Ad2 disassembly and DNA import *in vivo*. We next asked whether CAN/Nup214 is involved in

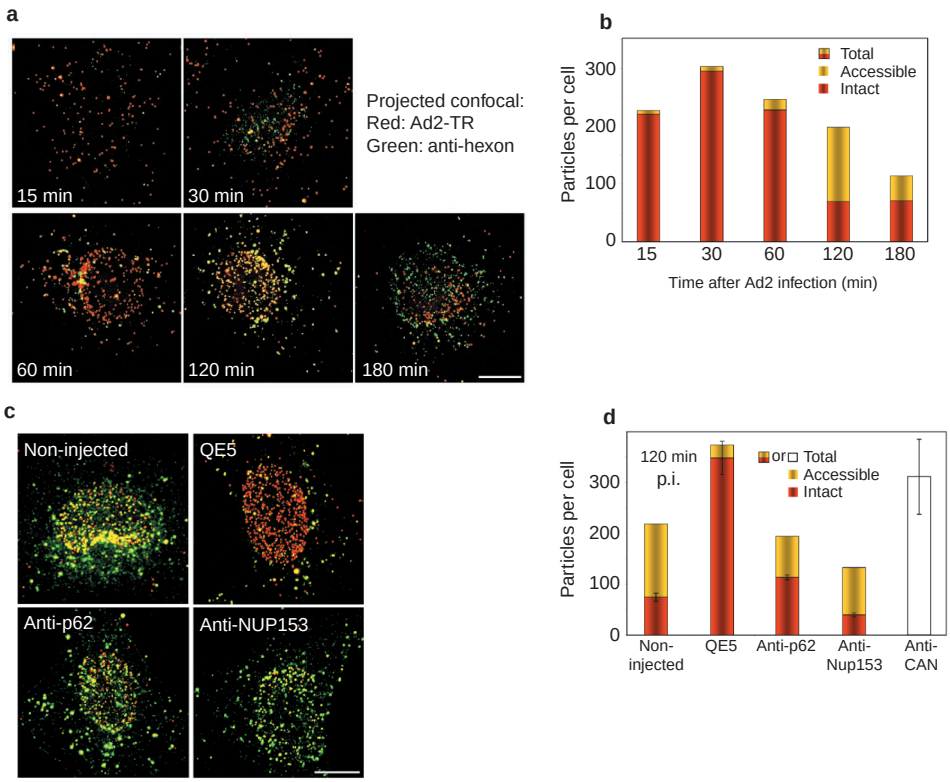

Figure 3 **Antibody-targeting to CAN/Nup214 interferes with Ad2 disassembly in A549 cells. a**, Progressive Ad2 disassembly can be visualized and quantified in single cells. A549 cells were infected with Ad2–TR (red) by cold binding and warming for indicated times, fixed and analysed by CLSM using a rabbit anti-hexon antibody (green). Projected entire CLSM stacks of Ad2–TR and hexon stainings were merged. Strong anti-hexon fluorescence indicates structural changes of the particles. **b**, Image quantification of **a**. All regularly sized Ad2–TR particles were counted with an automated routine in each optical section (total). Only anti-hexon negative particles were considered in a recount (red, intact) and the difference plotted as accessible (yellow, see also Methods). Most particles are intact at 60 min p.i., and become hexon-positive (accessible) at 120 min, and are uncountable fragments or aggregates of input virus at 180 min. Note that total particle counts are highest when single intact capsids are evenly distributed in the cytoplasm (30 min), or arrested at the nuclear membrane (QE5, see below). One typical experiment is shown. Additional examples of 120 min time points are provided in Figs 3d, 7A and D (noninjected). **c**, A549 cells were microinjected into the cytoplasm with the indicated antibodies, infected with Ad2–TR for 120 min and processed as described in **a**. Note that the mouse mAb QE5 prevented the appearance of hexon epitopes and irregular particles but apparently not Ad2–TR targeting to the nuclear membrane. **d**, Image quantifications of microinjected cells were performed as described in **b**, except that the rabbit anti-CAN antibody-injected cells could only be analysed for regular sized Ad2–TR particles and not for rabbit anti-hexon stainings (open box). Error bars are standard deviations of the mean ($n = 2$ to 4). Scale bar, 10 μm.

Ad2-infection of epithelial cells, and addressed events immediately downstream of the virus binding to the NPC, namely capsid disassembly and DNA import. Ad2 particles labelled with the fluorophore Texas Red (Ad2–TR) were used to trace individual viral particles. The TR label is incorporated exclusively into the major capsid protein hexon[19]. An antibody against hexon was used to assess particle intactness[5,20] and viral DNA localization by FISH (fluorescence *in situ* hybridization) analysis revealed successful nuclear import of viral genome[3]. The disassembly assay combines entry of Ad2–TR with immunofluorescence of the anti-hexon antibody that preferentially recognizes Ad2 capsids after disassembly[5]. Colocalization of this antibody (revealed by Alexa-488-labelled secondary antibodies) with Ad2–TR by single-cell confocal laser scanning microscopy (CLSM) analysis was used as an indicator of each particle's degree of disassembly and was verified by a time course experiment (Fig. 3a). At 15 and 30 min post infection (p.i.), intact Ad2–TR particles (in red) were distributed over the entire cellular area and only a few were recognized by the anti-hexon antibody. At 60 min p.i. most of the particles were still intact and localized to the nuclear periphery, but after 120 min they had become accessible to the anti-hexon antibody (green signal), which, on merging with the red channel (capsids), resulted in a yellow signal. At 180 min p.i capsids were found near the nucleus and in the cytoplasm, often as aggregates or fragments. To quantify capsid disassembly we determined the numbers for total (regular size Ad2–TR), intact (total minus hexon-positive) and accessible (that is, disassembled = total – intact) Ad2–TR particles with an automated counting routine (see Methods). We found that capsid disassembly was correlated with a large increase in accessible particle numbers between 60 and 120 min p.i., and a large decrease in countable capsids (the routine does not count particles of aberrant sizes — that is, capsid fragments and capsid clusters) typical of disassembled Ad2 (Fig. 3b). At 180 min p.i., the number of countable particles is reduced to ~30% of the number present at 30 min. These results are consistent with Ad2-disassembly kinetics in population assays[20].

The disassembly assay was next used to determine which anti-NPC antibodies, when microinjected into cells before infection, affected Ad2 disassembly. Our results indicate that QE5 almost completely abrogated Ad2 disassembly, as shown by the lack of yellow anti-hexon staining and the high number of intact Ad2–TR particles (Fig. 3c and d). Antibodies against p62 and Nup153 had no significant effect on disassembly compared with noninjected cells. The monospecific rabbit anti-CAN antibody strongly preserved countable particles, confirming that targeting of antibodies to CAN/Nup214 blocks Ad2 disassembly.

To verify whether CAN/Nup214 was required for DNA delivery

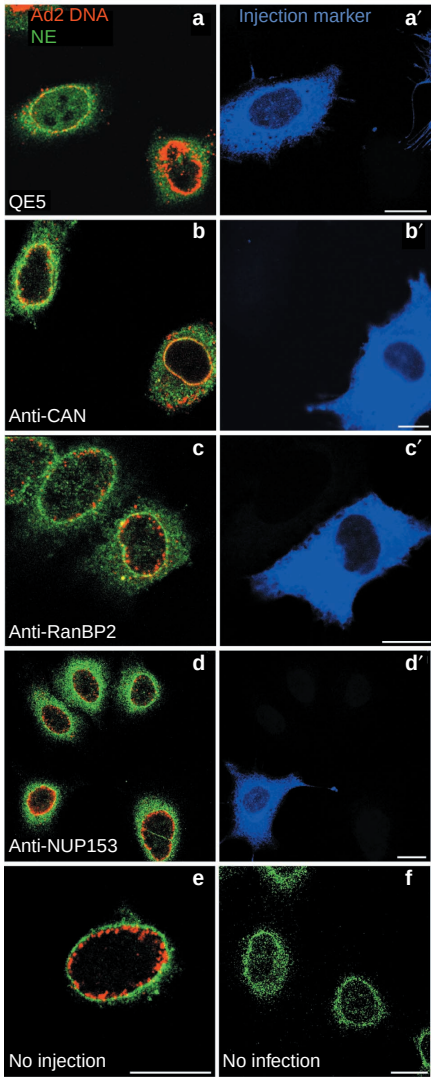

Figure 4 **Anti-CAN antibodies inhibit Ad2 import *in vivo*.** Cells were microinjected with the indicated antibodies in the presence of BSA–FITC (injection marker, pseudo-coloured in blue), infected with Ad2 for 3 h, fixed and processed for FISH assays with a TR-labelled Ad2 genomic DNA probe (red). The NPCs were stained with anti-CAN (**a**, **d**, **e**, **f**) or anti-p62 antibodies (**b**, **c**) and Cy5-conjugated secondary antibodies (pseudo-coloured in green). Single sections of each channel are shown at the position where the NE is perpendicular to the substratum. Note that the Ad2-DNA signal is at the nuclear rim in anti-CAN or QE5 antibody-injected cells (**a**, **b**) but clearly inside the nucleus in all other cases, including noninjected cells (**e**). Noninfected cells have no Ad2-DNA staining (**f**). All images are representative of multiple independent experiments. Scale bar, 10 μm.

into the nucleus, we monitored the viral DNA signal by FISH. As expected[3], viral DNA was localized inside the nucleus of noninjected control cells at 180 min p.i., consistent with earlier findings (Fig. 4e and f, ref. 2). Cells injected with either QE5 or anti-CAN antibodies, however, did not import viral DNA but seemed to enrich the incoming DNA at the nuclear membrane (Fig. 4a, b, a′ and b′). In contrast, the RanBP2 and Nup153 antibodies (Fig. 4c, d, c′ and d′) did not affect DNA import. These results demonstrate that disassembly and DNA import are inhibited by antibody targeting to CAN/Nup214 *in vivo*, and are consistent with a function for CAN in Ad2 attachment to the NPC.

Histone H1 binds the Ad2 capsid protein hexon. In a search for additional proteins involved in nuclear events of the adenoviral infection process, purified Ad2 was incubated with low-salt NE extracts, followed by viral sedimentation through sucrose gradients. In the absence of salt extract, Ad2 migrated to the middle fraction of the gradient (Fig 5a, lane Ad2, and Fig. 5b, Ad2 alone), but after incubation with NE extract Ad2 was quantitatively pelleted, as indicated in silver-stained SDS–polyacrylamide gel electrophoresis (PAGE) (Fig. 5a, lane Pel) and quantitative sedimentation profiling of [^{3}H]-thymidine-labelled Ad2 and [^{35}S]-methionine-labelled Ad2 (Fig. 5b). Two protein bands from the NE extract co-sedimented with Ad2 (Fig. 5a). Purification of the major band by ion-exchange chromatography and high-performance liquid chromatography (HPLC) to homogeneity and subsequent analysis by matrix-assisted laser desorption ionization (MALDI) mass spectrometry yielded an M_r of 21,913. The amino-acid composition of this protein suggested that it was the mono-acetylated rat isoform of histone H1.2, which has a predicted mass of 21,898. We confirmed this result by western blotting using a monoclonal anti-H1 antibody (Fig. 5a). The minor lower band was later identified as another histone H1 variant (revealed by amino-acid analysis of the HPLC-purified protein; data not shown). Notably, none of the core histones present in the NE salt extract (Fig. 5a, Extr.) bound to Ad2. Using Ad2–SSBED, we next asked whether H1 binding could also occur during Ad2–NPC docking. Ultraviolet illumination of Ad2–SSBED alone crosslinked mainly hexon, penton base and fibre proteins (Fig. 5c, lane 2). But when NPC-bound Ad2–SSBED was illuminated with ultraviolet light, biotin was consistently transferred to histone H1, as indicated by anti-biotin and anti-H1 western blotting (Fig. 5c, lanes 3 and 6). Quantification of the SSBED distribution on the capsid by nonreducing SDS–PAGE and western blotting of virus not treated with ultraviolet radiation showed that more than 93% of the crosslinker was attached to hexon and less than 7% was on fibre. Taken together, these results indicate that NPC-bound particles can bind histone H1, and that H1-binding occurs via hexon. Because anti-H1 antibodies had no effect on Ad2 binding to NEs (Fig. 2a), we concluded that H1 is not required for NPC binding.

H1 linker histones contain a conserved globular domain[21] flanked by two flexible lysine-rich tails that are thought to interact with the poly-phosphate backbone of DNA, and are essential for chromatin folding and condensation[22]. Ad2 hexon contains a cluster of 16 acidic residues in one of its surface loops[23]. This cluster is highly abundant (720 copies per virion) and is conserved among subgroup C but not subgroup B adenoviruses (Fig. 6). We therefore tested whether rat H1.2 was able to pellet the subgroup B virus Ad3. Incubation of [^{3}H]-Ad3 with purified rat H1.2 at 4 °C did not result in pelletable Ad3, nor did a 10× excess of unlabelled Ad3 prevent pelleting of [^{3}H]-Ad2 with H1.2. [^{3}H]-Ad2 pelleting with H1.2 was, however, competed by 10× excess of unlabelled Ad2, indicating that H1 only binds Ad2 (Fig. 5d). Moreover, DNase treatment of [^{3}H]-Ad2 did not inhibit H1.2-induced Ad2 pelleting nor did it release [^{3}H]-thymidine from the particles, indicating that viral DNA remained protected (data not shown). We conclude that H1 probably binds to the surface-exposed acidic clusters of Ad2 hexon.

Nuclear H1 is required for Ad2 disassembly and DNA import. We examined whether H1 is involved in Ad2 import. Two different anti-H1 antibodies were injected into the nuclei of A549 cells to directly access the vast nuclear pools of H1. The first reagent was the anti-H1 monoclonal antibody (mAb) used in the previous binding experiments (Fig. 2a) and for the colocalization experiments discussed in the next section. Nuclear microinjection of the anti-H1 mAb strongly reduced Ad2 disassembly, as measured by the disassembly assay. There were no significant effects observed in noninjected cells or nuclear control injections (Fig. 7A), nor in cells cytoplasmically injected with anti-H1 mAb (data not shown). This antibody also inhibited import of Ad2 DNA but again, only if injected into the nucleus (Fig. 7B, a, a′

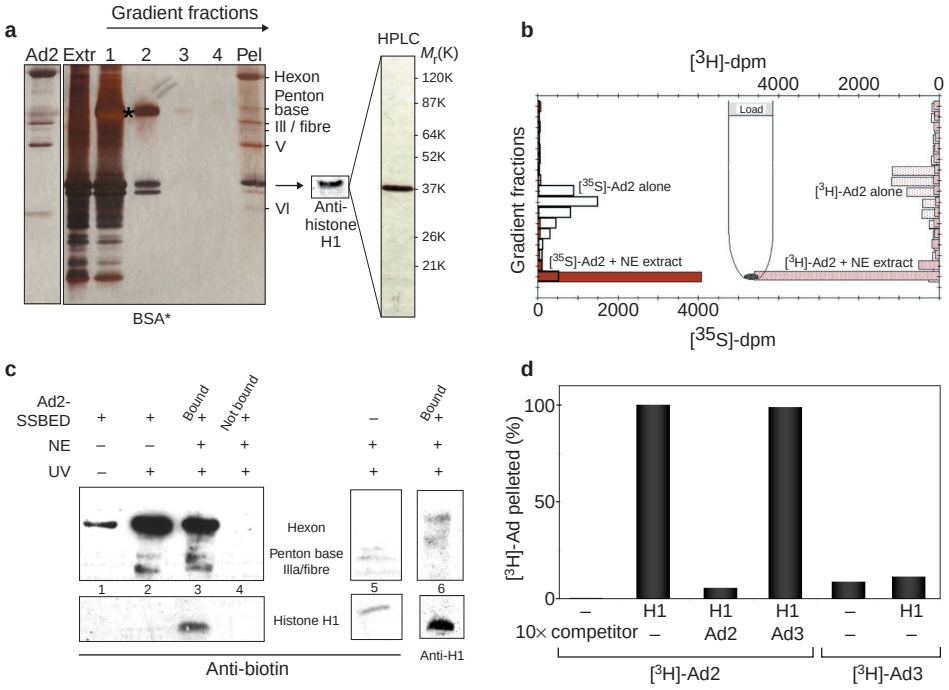

Figure 5 **Histone H1.2 binds Ad2 *in vitro* and *in vivo*. a**, Ad2 (6 μg) was incubated with a 0.25 M NaCl extract of NEs (0.05 ml, 2 OD_{260} equivalents) at 4 °C for 30 min and centrifuged in a sucrose-density gradient so that Ad2 alone migrated to the middle of the gradient (see Ad2 lane). Fractions including the pellet (Pel) were analysed by SDS–PAGE and Ad2 was found in the pellet. In addition to the viral proteins (hexon, penton base, IIIa, fiber, V and VI) the pellet contained two bands present in the extract (Extr.) and the top fractions. The dominant band was purified to homogeneity by HPLC. The arrow shows a western blot of a pellet lane with anti-histone H1 antibody. **b**, [3H]-thymidine or [35S]-methionine-labelled Ad2 was reacted with NE extract, subjected to sucrose gradient centrifugation and fractions were analysed by liquid scintillation counting as described in Fig. 1a. **c**, NE-bound Ad2 crosslinks histone H1. Ad2–SSBED was incubated with NEs at 4 °C for 45 min. NEs were pelleted through sucrose, ultraviolet illuminated, analysed by reducing SDS–PAGE and western blotted with anti-biotin antibodies. Transfer of biotin to H1 was obtained with NE-bound Ad2 (lane 3) and confirmed with anti-H1 blotting (lane 6). NEs alone had minimal reactivity to the anti-biotin antibody (lane 5). Nonultraviolet-illuminated Ad2–SSBED indicates a small degree of background crosslinking (lane 1), whereas ultraviolet-illuminated Ad2–SSBED shows predominant intraviral hexon crosslinking and some crosslinking of penton base and fiber proteins (lane 2). Note that NPC proteins (for example, CAN/Nup214) are not detected in this assay. **d**, Histone H1 pellets Ad2 but not Ad3. Purified H1 (0.1 μg in 0.05 ml) was incubated with [3H]-Ad2 (0.15 μg) or [3H]-Ad3 (0.15 μg) in the presence or absence of unlabelled competitor (10× excess) at 4 °C for 30 min and centrifuged. [3H]-d.p.m. of gradient and pellet fractions were determined as in Fig. 1a.

and b). Nuclear injection of the second reagent, a polyclonal affinity-purified rabbit anti-H1 antibody[24], also strongly inhibited import of Ad2 DNA measured at 180 min p.i. (data not shown). Nuclear injections of antibodies against histone H4 or phosphorylated H1 (which is present in low amounts) had no effect (Fig. 7B, c, d), indicating that antibody targeting to the major nuclear population of H1 specifically interfered with Ad2 disassembly and, consequently, DNA import. Notably, inhibiting protein synthesis with cycloheximide had no apparent effect on Ad2 disassembly and DNA import[3], thus confirming the requirement of pre-existing (nuclear) H1. Importantly, the anti-H1 mAb had no effect on DNA import of Ad3 measured at 7 h p.i. (that is, the time required for efficient Ad3-DNA import), but still inhibited Ad2-DNA import, albeit to a lesser extent than at 3 h p.i. (Fig. 7C). These data suggest that nuclear H1 is required for Ad2 disassembly, presumably by binding to hexon. Moreover, it is unlikely that H1 is involved in Ad3 disassembly and DNA import.

Histone H1 colocalizes with disassembled Ad2 capsids *in vivo*. To determine whether H1 interacts with Ad2 before the disassembly process, we infected TC7 cells with Ad2–TR for 30 and 120 min. We did not detect any cytoplasmic colocalization of intact incoming Ad2–TR with anti-H1 mAb at 30 min p.i. (Fig. 8, projection of entire confocal stacks). At 120 min, after the majority of Ad2 capsids had disassembled, we did, however, observe a significant and reproducible amount of the resulting cytoplasmic Ad2–TR capsid fragments colocalizing with histone H1 (Fig. 8, projection of six optical confocal sections). Together, these data suggest that H1 does not associate with Ad2 before the process of capsid disassembly.

Impβ and importin 7 (Imp7) are involved in Ad2 disassembly. Because histone H1 was able to contact hexon at the NPC *in vitro*, we tested whether nuclear import factors of H1 were involved in Ad2 disassembly. Using a microinjection approach, we targeted the two known H1-import factors, Impβ and Imp7 (ref. 25). Both anti-Impβ and anti-Imp7 antibodies effectively interfered with Ad2 disassembly, as indicated by the disassembly assay (Fig. 7D). Both of these antibodies also blocked import of viral DNA into the nucleus measured at 180 min p.i. Antibodies against CRM1, another importin family member, had no effect on Ad2-DNA import and did not interfere with Ad2 disassembly (Supplementary Information Fig. S2 and Fig. 7D, respectively). This suggests that the inhibition of disassembly by Impβ and Imp7 antibodies was not due to nonspecific effects on trafficking through nuclear pores. Instead, the H1-import factors might facilitate the translocation of H1–hexon complexes into the nucleus, which could be sufficient to drive the conformation of the 'intact' capsid to an accessible capsid, ready to release its DNA (Fig. 9).

Discussion

A viral capsid accomplishes multiple tasks, including surface docking, membrane penetration and cytoplasmic transport[26,27]. Priming

```
Sub-
group
        Ad1  ......... .........A YNALAPKGAP NSCEWEQEEP TQEMAGELED EE.EAEEEEA EEEAEAPQAG QKVKKTHVYA QAP...LAGE KITANGLQIV
C       Ad2  FDIRGVLDRG PTFKPYSGTA YNALAPKGAP NSCEWEQTED SGRAVAEDEE EEDEDEEE.. .EEEEQNARD QATKKTHVYA QAPL...SGE TITKSGLQIG
        Ad5  FDIRGVLDRG PTFKPYSGTA YNALAPKGAP NPCEW...DE AATALEINLE EEDDDNED.. .EVDEQAEQQ ....KTHVFG QAPY...SGI NITKEGIQIG
        Ad6  ......... .........A YNALAPKGAP NSCEWEQNET AQVDAQELDE EENEANEAQA REQEQA.... ...KKTHVYA QAP...LSGI KITKEGLQIG

        Ad3  FDIRGVLDRG PSFKPYSGTA YNSLAPKGAP NTSQWIVTTN GDNAVTT... ......... ......... ....TTNTFG IASM...KGD NITKEGLQIG
B       Ad7  FDIRGVLDRG PSFKPYSGTA YNSLAPKGAP NTSQWIVTAG EERAVTT... ......... ......... ....TTNTFG IASM...KGD NITKEGLEIG
       Ad16  FDIRGVLDRG PSFKPYSGTA YNSLAPKGAP NTCQW..... ..KDSDS... ......... ......... ....KMHTFG VAAMPGVTGK KIEADGLPIG
```

Figure 6 **Ad2 but not Ad3 hexon contains a subgroup-specific acidic cluster.** Alignment of hexon sequences from human Ad serotypes of subgroups C and B reveals a cluster of 16 surface-exposed acidic amino acids in Ad2[23] but not in subgroup B hexons of Ad3, Ad7 and Ad16.

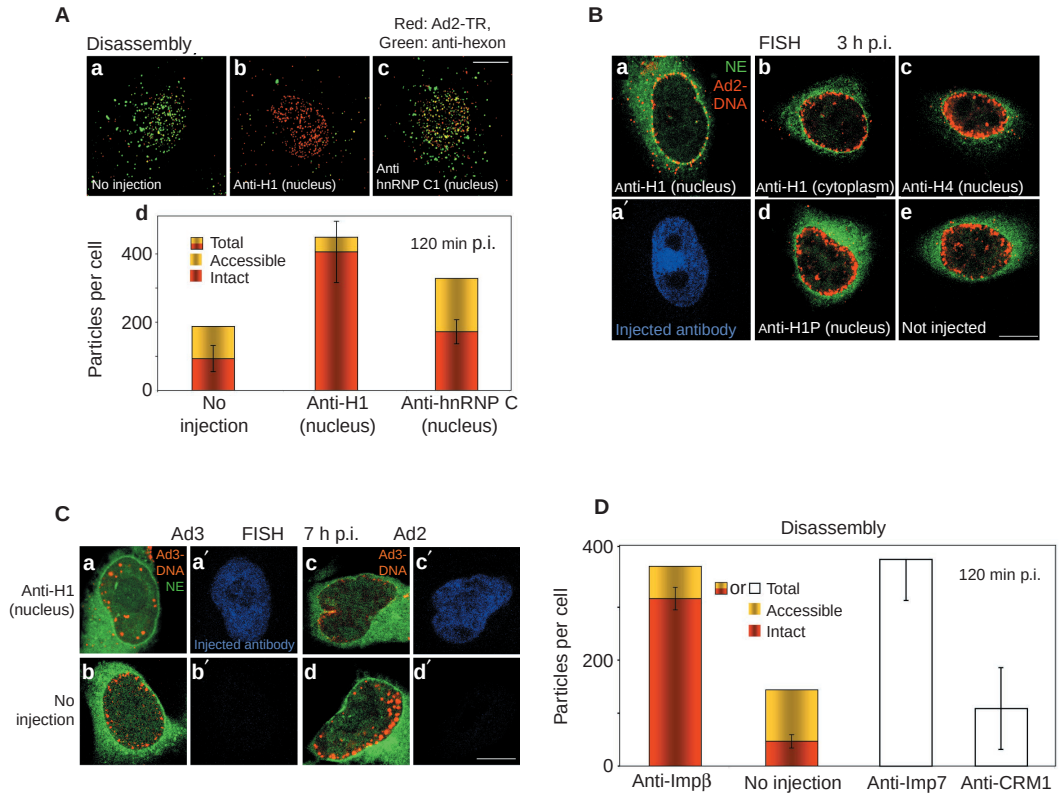

Figure 7. **Anti-histone H1 antibodies inhibit Ad2 disassembly and nuclear import of DNA in A549 cells. A**, Nuclei were injected with anti-histone H1 or anti-hnRNP C1 control antibodies and cells infected with Ad2–TR for 2 h (**a–c**) and processed for anti-hexon immunofluorescence and image quantification (**d**). Injection sites were verified by anti-immunoglobulin-γ (IgG) stainings. Error bars depict standard deviations ($n = 4$). **B**, Cells were microinjected into the cytoplasm or the nucleus with antibodies as indicated and infected with Ad2 (3 μg) for 3 h. Ad2 DNA was visualized by FISH using a TR-labelled viral DNA probe (**a–e**, red signal). The NPCs were stained with anti-CAN and Alexa 350 conjugated anti-rabbit antibodies (**a** and **b**, green pseudo-colour) or anti-p62 and Alexa-350-conjugated anti-mouse antibodies (**c**, **d**, **e**). Injected cells were identified by co-injected BSA–FITC (data not shown). Injection sites were verified by visualizing injected antibodies with anti-mouse or rabbit IgG conjugated to Cy5, of which one example is shown (**a′**, anti-mouse IgG, blue pseudo-colour). Single CLSM sections were analysed as described in Fig. 4. Results are representative of multiple independent experiments. **C**, Anti-histone H1 antibodies do not affect nuclear import of Ad3 DNA. Nuclei of A549 cells were injected with anti-H1 antibodies (**a** and **c**) or not injected (**b** and **d**) and cells infected with Ad3 (3 μg per assay, **a** and **b**) or Ad2 (3 μg per assay, **c** and **d**) for 7 h, fixed and processed for FISH analysis. Injected antibodies are shown in (**a′–d′**). Results are typical of two independent experiments. **D**, Targeting of antibodies to histone H1-import factors interferes with Ad2 disassembly. Cells were injected into the cytoplasm with a mouse anti-Impβ mAb or rabbit anti-Imp7 or anti-CRM1 antibodies (as control) and infected with Ad2–TR for 120 min. Anti-Impβ and noninjected cells were processed as described in Fig. 3b and cells injected with rabbit antibodies were quantified for regular particles as described in Fig. 3d (open boxes). Error bars indicate s.d. ($n = 4$). Scale bar, 10 μm.

the capsid for nuclear import must be regulated to prevent interference with earlier steps of entry. Priming can, for example, be achieved by loss of components to uncover binding sites, as has been suggested for the herpes simplex virus (HSV)-1 capsid, which loses tegument proteins[28], or by phosphorylation of capsid proteins (for example, of human hepatitis B virus)[1]. In each of these cases, priming could allow interactions with import factors and thus promote nuclear import. Our findings now suggest a new two-step mode of virus–NPC interactions. In the first step, nonclassical binding to fibrils ensures stable NPC localization during the slow disassembly and import processes. In the second step, accumulation of import factors on the particle initiates partial opening of the capsid. In the case of Ad2, the capsid docks to the NPC filament protein CAN/Nup214 and positions itself to accumulate the mobile

nuclear protein histone H1 and subsequently H1-import factors Impβ and Imp7, priming the capsid for disassembly.

Nonclassical binding of Ad2 to NPCs via CAN/Nup214. Although all newly synthesized structural adenoviral proteins are inherently able to enter the nucleus (where particles assemble about 24 h p.i.), and probably rely on soluble import factors[29], Ad2 binds to rat liver NEs independently of additional cytosolic factors, unperturbed by high levels of the Ran–GTP analogues Ran–GMP-PNP or Ran–GDP. These results imply that Ad2 has an intrinsic capacity for docking to the NPC. This binding was not obstructed by antibodies against RanBP2 or Impβ, but by antibodies against C-terminal CAN/Nup214 epitopes and also by soluble RNPs. Furthermore, we confirmed a direct interaction by crosslinking Ad2–SSBED to the C terminus of CAN/Nup214 *in vitro*. This domain contains characteristic FG repeats and binds to the export receptor CRM-1 (ref. 30). Whether Ad2 competes with CRM-1 for CAN binding, and whether Ad2 can bind to FG repeats of other proteins *in vitro* is unknown. Interestingly, CAN/Nup214 may also function as a docking site for import of U1 snRNPs, before the snRNPs engage with the import factor snurportin1 (N. Panté, personal communication, and ref. 31). CAN/Nup214 is also an important binding site for Ad2 *in vivo*, as suggested by the fact that the events immediately downstream of NPC binding, disassembly and DNA import were strongly blocked by all of our CAN/Nup214-recognizing antibodies. Additional NPC-binding sites may contribute to Ad2–NPC binding but they seem to be insufficient for supporting Ad2 disassembly and DNA import.

Histone H1 mediates Ad2 disassembly. By screening salt extracts of rat liver NEs for Ad2-binding proteins we initially isolated rat histone H1.2. This variant (also termed H1.d) is expressed in somatic tissue, including epithelial cells[32]. It is highly homologous to human H1.2 and closely related to the mouse variants H1.0 and H1.c (ref. 33). Binding of rat liver H1.2 to Ad2 caused viral pelleting after centrifugation. This probably occurred because of direct interactions with Ad2 capsid hexon proteins, as indicated by crosslinking experiments. Because the interaction was insensitive to nucleases, we have ruled out the possibility that H1 contacts Ad2 DNA. Because polylysine can substitute for histone H1 in pelleting Ad2, we think that, *in vitro*, rat H1.2 acts as a bivalent crosslinker of Ad2, bridging capsids with its two polylysine-like tails. Although H1 histones are known to bind a variety of proteins in a nonspecific fashion, our data suggest an interaction that is specific for the surface-exposed acidic cluster found in the hexon protein of Ad2 but not that of Ad3 (Fig. 6). Of the seven hypervariable regions (HVRs) in Ad2 hexon, only three are highly conserved between the subgroups. Although it is assumed that they account for some subgroup-specific differences, so far no functions in Ad entry have been assigned to any of these regions. We propose that one function of the acidic cluster of HVR1 is to bind histone H1.

Viral particles that are larger than the size limits of the NPC require capsid disassembly before genome import. This has been shown, for example, for Ad2 and HSV-1[20,28]. Microinjections of anti-H1 antibodies into cell nuclei inhibited Ad2 disassembly as efficiently as antibodies that interfered with binding of Ad2 to the NPC. Because H1 binds directly to intact capsids *in vitro* and colocalized with Ad2 only after, and never before, disassembly *in vivo*, we suggest that, after stable attachment, the last step of Ad2 DNA

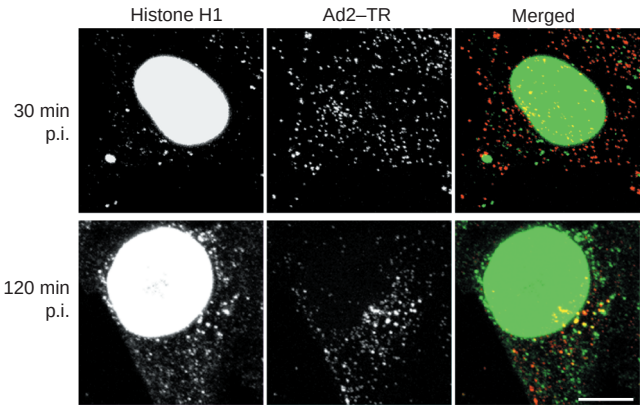

Figure 8 **Histone H1 and Ad2–TR colocalize after virus disassembly.** TC7 cells were infected with Ad2–TR (red) for 30 or 120 min and processed for anti-histone immunofluorescence (green). A projection of the entire optical stack is shown for the 30 min time point and six subsequent sections from the middle of the cell are shown at 120 min p.i. Yellow signals at 120 min p.i. indicate overlapping stainings of Ad2–TR and H1. Each overlap was verified in the appropriate single section. Scale bar, 10 μm.

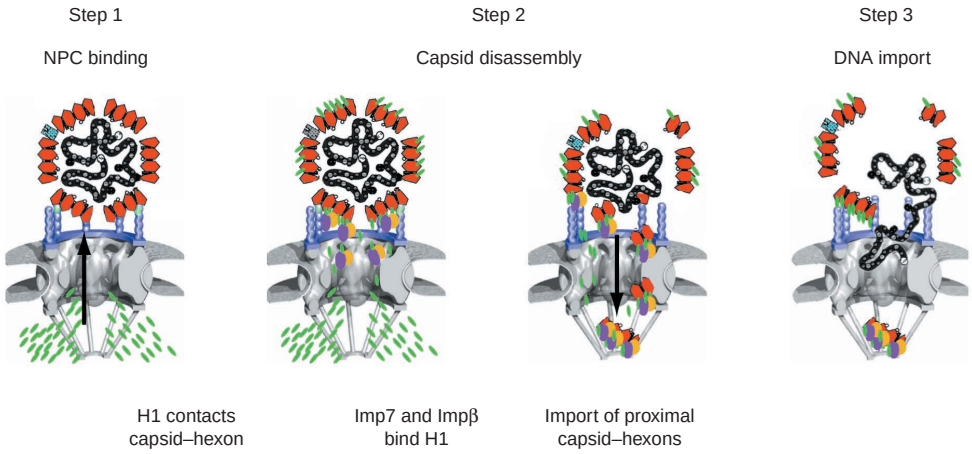

Figure 9 **Model for Ad2 disassembly and DNA import.** A partly weakened Ad2 particle arrives at the nuclear membrane and docks to the NPC-filament protein CAN/Nup214. The proximity of the Ad2 capsid to the nuclear pore allows binding of hexon to dynamic histone H1 (step 1). The H1-import factors Impβ and Imp7 then initiate capsid disassembly via histone–hexon import (step 2). This enables import of DNA through the nuclear pore. Nuclear import signals on the viral chromatin proteins and/or histone H1, and possibly additional factors, then mediate translocation of DNA into the nucleus (step 3).

delivery into cells is initiated by direct binding of nuclear histone H1 to capsid hexon proteins. Because the decisive factor, histone H1, is not abundant in the cytoplasm, its accumulation on the weakened cytosolic capsid preferentially occurs near the nucleus. The requirement of H1-import factors further indicates that disassembly occurs on functional NPCs. Because the purification of the weakened cytosolic Ad2 particle has remained elusive so far, it is not known whether additional factors are required for Ad2 disassembly.

A model for Ad2-DNA import. Binding of an NLS-bearing protein cargo to an import receptor is sufficient for rapid import into the cell nucleus. NLSs have been identified on numerous viral capsids including HIV-1 pre-integration complexes[1], plant viral capsids[34] and hepadna viruses[35,36]. Our findings now suggest an additional requirement for import that is shared by snRNPs, namely, stable NPC attachment via CAN/Nup214. The partially weakened cytosolic Ad2 capsid arrives at the NPC and docks via CAN/Nup214 (Fig. 9). Only the CAN-docked particle (which is about a thousand times larger than a typical protein cargo) can, in a second step, engage the classical receptor-mediated import pathway. By virtue of its acidic surface clusters, Ad2 accumulates nuclear histone H1. H1 is a nuclear protein at steady state and binds dynamically, rather than stably, to chromatin, thus allowing small amounts of H1 to escape from the nucleus[37,38]. Normally, cytosolic H1 is efficiently retrieved by the H1-import system[25]. We thus propose that the H1-import factors Impβ and Imp7 recognize H1 on docked Ad2 capsids and induce import of the most proximal H1–hexon complexes (about 5% of incoming hexon[5]). This is consistent with the observation that Ad-DNA import in digitonin-permeabilized cells requires soluble factors, in addition to importin α (Impα), Impβ, NTF2 and Ran[39]. Importantly, an NPC-restricted, CAN-facilitated disassembly process ideally positions the viral DNA for import. If CAN/Nup214 turns out to be a docking site for other viruses, it may be used as a novel target for therapeutic interventions against viral infections. □

Methods

Cells, viruses and proteins

Human lung carcinoma A549 cells were maintained in Dulbecco's modified Eagle's medium (DMEM supplemented with 7% semi-synthetic serum clone III; Hyclone) and placed on alcian-blue-coated glass coverslips at least 48 h before experiments[40]. Ad2 was grown and labelled with [^{3}H]-thymidine[5], and infections were carried out by cold synchronisation[3]. Ad3 was obtained from S. Hemmi. The following antibodies were generous gifts from various investigators. Mouse mAb QE5 against p62, Nup153 and CAN/Nup214 (N. Panté and B. Burke[13]), mAb SA1 against Nup153 (B. Burke[18]), mAb 3E9 against importin β (S. Adam[15]), mAb 4F4 against hnRNP C1 (G. Dreyfuss[41]), RL-1 and RL-2 against O-linked nucleoporins and RL27 against gp210 (L. Gerace[11,17]). Rabbit antisera used were directed against Ran BP2 (antibody 551, T. Nishimoto[42]), Imp7 (affinity purified, D. Görlich[25]), Ad2 hexon (M. Horwitz, as described in ref. 5), the C terminus of CAN/Nup214 and CRM1 (G. Grosveld[14,30]). Rabbit anti-H1 antibodies obtained from M. Bustin (NIH, USA) were elicited against calf-thymus histone-H1 subfractions[43] and affinity purified on Sepharose-4B-immobilized histone H1 (ref. 24). Commercial mouse mAbs were against histone H1 (Upstate Biotechnology) and p62 (Transduction Laboratories). Goat antibodies against biotin coupled to horseradish peroxidase were from Sigma, goat IgG against mouse IgG coupled to Alexa 350 (blue), 488 (green) and 594 (Texas Red) were from Molecular Probes and goat anti-mouse coupled to Cy5 (near-infra red) were from Jackson Laboratories. Rabbit anti-phosphohistone H1 and anti-histone H4 were obtained from Upstate Biotechnology.

Ran/TC4 was expressed in *Escherichia coli* and purified as described previously (with an expression plasmid from F. Melchior[44]). The His-tagged C terminus of CAN (residues 1,549–2,090) was expressed from plasmid pRSET-B-hCAN (1,549–2,090) that contains the *Psh*AI–*Eco*RI fragment of the human CAN/Nup214 complementary DNA in the *Pvu*II and *Eco*RI sites of pR-SET-B (Invitrogen) in BL21:DE3:pLysS, and purified using Ni^{2+}-nitrilotriacetate–agarose (Qiagen) under denaturing conditions (8 M urea) and slowly dialysed to 250 mM NaCl, 20 mM HEPES–KOH buffer at pH 7.9, 8.7% glycerol. An *E. coli* extract containing GST and minor amounts of unknown proteins was used as control. FITC–BSA–NLS was prepared using earlier protocols[3,15] and contained 20 SV40-large T-NLS peptides per molecule (a gift of O. Meier, University of Zurich).

In vitro binding assays

Rat liver NEs were prepared as described previously[11], except that DNase and RNase (10 μg ml^{-1} each) treatments were carried out in STKM buffer (0.25 M sucrose, 10 mM Tris–HCl buffer at pH 7.4, 100 mM KCl, 1 mM $MgCl_2$ containing protease inhibitors) at 4 °C for 45 min. [^{3}H]-Ad2 (0.06 μg of 0.3 μg μl^{-1}, 420,000 d.p.m. μg^{-1}) was incubated with 3–6 × 10^5 equivalents of rat liver NEs[11] at 4 °C for 30 min. NE-bound virus was separated from unbound virus by centrifugation through a sucrose step gradient (0.25 ml 20%, 0.5 ml 30%, 0.15 ml 80% sucrose in STKM) for 10 min at 4 °C and 6,650g_{av} in a TLS-55 swing-out rotor of a TLX table-top ultracentrifuge (Beckman). Fractions including the pelleted material were collected from the top, denatured with SDS (0.1–0.2% final concentration), mixed with a 12-fold excess of Ready-Safe liquid scintillation cocktail and [^{3}H]-dpm determined in an LS 3801 scintillation counter (Beckman). Inhibition experiments were carried out by preincubating NEs with antibodies at 4 °C for 1 h at a 1000× excess of antibody over NPCs (estimating 3,000 NPCs per NE) or, in the case of Ad2 capsid protein competition, a 100× excess of purified protein over Ad2 protein, followed by incubation with appropriate amounts of [^{3}H]-Ad2 to yield a 50–70% binding efficiency in control samples. RNP-inhibition experiments of Ad2-binding to NEs were carried out with rabbit reticulocyte RNPs or RNase-treated RNPs (1 μg ml^{-1} RNase, 30 °C, 30 min) as described above. Ran–GDP was loaded with the nonhydrolysable GTP analogue GMP-PNP by incubating 10 μM Ran–GDP with 1 mM GMP-PNP in 25 μl LB (50 mM HEPES–KOH at pH 7.4, 1 mM magnesium acetate, 10 mM EDTA, 2.5 mM dithiothreitol and 1 mM ATP) for 45 min at room temperature. NEs ($2D_{260}$; that is, 6 × 10^6 nuclear equivalents) were suspended in this solution or in LB containing 10 μM Ran–GDP for 1 h at room temperature and FITC–BSA–NLS was added to 0.5 mg ml^{-1}. After incubation at 4 °C for 45 min aliquots were removed for fluorescence microscopy as described in ref. 3. [^{3}H]-Ad2 (0.15 μg) was added to the remaining samples and analysed for binding to NEs as described above.

Ad2–H1 pelleting assays were performed by incubating Ad2 (6 μg) or [^{3}H]-Ad2 (0.06–0.24 μg) with rat histone H1.2 (10–100 ng) in the presence or absence of indicated amounts of competitors in STKM at 4 °C for 30 min, followed by a sucrose-density step centrifugation (0.3 ml of each 10%, 20% and 30% sucrose in STKM) at 60,000g_{av} for 10 min as described above. Gradient fractionation and scintillation counting were carried out as described above and analysed by reducing SDS–PAGE in a 10–15% acrylamide gradient gel.

Ultraviolet crosslinking

Ad2–SSBED was prepared by incubating CsCl-purified Ad2 with Sulfo-SBED (sulfo-N-hydroxysuccinimido 2-[6-(biotinamido)-2-(p-azidobenzamido)-hexanoamido]ethyl-1,3-dithioproprionate; Pierce, 33033) at a 4:1 weight excess of Ad2, as described for Ad2 labelling with TR[19]. The reaction product (Ad2–SSBED) had the same infectivity (plaque-forming units on A549 cells) per weight as the non-modified Ad2. C terminus of CAN/Nup214 (1 μg) or crude control mix was incubated with Ad2–SSBED (3 μg) for 30 min at room temperature in 10 mM Tris–HCl at pH 7.4, 250 mM NaCl in 50 μl. NEs ($0.9D_{260}$) were incubated with Ad2–SSBED (3 μg) in 50 μl STKM buffer at 4 °C for 30 min, pelleted through sucrose and resuspended in 50 μl STKM. All samples were transferred onto parafilm and ultraviolet irradiated (366 nm, 16 W, 5 cm lamp–sample distance) on ice for 15 min. The samples were reduced with 100 mM β-mercaptoethanol, subjected to SDS–PAGE and western blotted, stained with Ponceau S, washed, incubated with anti-biotin and anti-H1 antibodies in the presence of 5% BSA (fraction V, Fluka) and analysed by enhanced chemiluminescence (Amersham).

Purification of histone H1, RNPs and Ad2 capsid proteins

Rat liver NEs were incubated with STKM containing 0.125 M NaCl at 4 °C for 15 min and membranes were pelleted (10,000*g*, 15 min). The supernatant was dialysed against TKM (STKM without sucrose) at pH 7.4, and 1 ml was run over a Mono-Q anion-exchange column (5 ml bed volume, 1 ml min^{-1}, BioLogic System, BioRad). The nonbound fraction was recovered (1 ml) and a 0.05-ml aliquot was applied to a μRPC C2/C18 reversed-phase HPLC column equilibrated in 0.05% trifluoroacetic acid (TFA) and eluted in a linear gradient of 95% acetonitrile/0.05% TFA at about 35% acetonitrile/0.05% TFA (SMART System, Pharmacia). Fractions were analysed by SDS–PAGE and homogeneous fractions of about 30 ng protein were subjected to MALDI mass spectrometry (P. James, the Laboratory for Protein Chemistry of the ETH Zurich). Total amino-acid analysis of about 60 ng of purified protein was done by P. Hunziker (University of Zurich). Amino-acid composition and mass were compared against the SWISS-PROT library using ExPASy (http://www.expasy.ch) and the protein assigned to histone H1.2 following the nomenclature of the original gene sequence publication (SWISS-PROT Prot primary accession number P15865, and ref. 45). RNPs were purified from 15 μg RNase-free rabbit reticulocyte lysate (Promega) by Sephadex G6 gel-filtration chromatography (BioLogic Chromatography System, BioRad) and recovered in the flow through. Ad2 capsid proteins were recovered from the top fraction of CsCl density gradients used for purification of Ad2 particles[5], supplemented with protease inhibitors, dialysed against 40 mM Tris–HCl at pH 7.4, centrifuged in a TLS-55 rotor (Beckman, 100,000*g*, 2 × 30 min) and fractionated on a Mono-Q anion-exchange column (BioLogic, BioRad) by elution in a linear NaCl gradient (0–1 M, 1 ml min^{-1}). Fibre was recovered in the flow through; penton base eluted at 0.2 M NaCl and hexon at 0.3 M NaCl. The fractions had an estimated Coomassie Blue SDS–PAGE purity of 98% for hexon and about 50% for penton base and fibre, respectively.

Microinjections, disassembly and FISH assays

A549 cells were microinjected with a mixture of antibodies (0.5 mg ml^{-1}) and FITC-labelled BSA (injection marker) in MI buffer (0.12 M KCl, 0.01 M Tris–HCl at pH 7.4), as described previously[3]. After recovery (37 °C for 30 min) cells were incubated in the cold with Ad2–TR (2 μg) or unlabelled Ad2 (3 μg) for 45 min and warmed at 37 °C as indicated. For indirect immunofluorescence analysis, cells were fixed in 3% paraformaldehyde and stained with primary antibodies overnight. Visualization with secondary antibodies was as follows: goat anti-rabbit Cy5-labelled antibody (GAR-Cy5) for labelling hexon in the disassembly assay. In the FISH assay, nuclear injections were verified by goat anti-mouse coupled to Cy5 (GAM-Cy5) or GAR-Cy5 antibodies (Amersham); cell integrity controlled by differential-interference contrast (DIC) sampling and nuclear-envelope stainings were visualized by Alexa 350 GAR or GAM antibodies (Molecular Probes) in quadruple labellings. Cells were mounted in paraphenylene diamine (0.5%), glycerol (80%), Tris (20 mM) at pH 8.8. Effect of antibodies on FITC–BSA–NLS import was verified as above but injections and recovery were performed at 4 °C to prevent FITC–BSA–NLS import and allow binding of injected antibody. Import was scored after incubating samples at 37 °C for 20 min.

Confocal images were recorded on a Leica SP1 microscope (63× oil-immersion objective) using ultraviolet excitation at 351 and 364 nm, FITC 468, TR 568, Cy5 647 and long-pass emission filters in sequential recording mode at a section thickness of 0.5 μm and with a constant zoom factor for each experimental series. Apparent particle numbers were counted in batch-processed stacks of Ad2–TR (Adobe Photoshop, Adobe Systems) using the public domain NIH Image program (developed at the US National Institutes of Health and available on the Internet at http://rsb.info.nih.gov/nih-image). Regular Ad2–TR particles were scored using the typical area of an Ad2–TR particle described

previously[19]. This number was defined as total particles, but was probably a slight overestimate of the actual number of objects due to multiple counting of the same particles in different optical sections. In addition, the routine did not count individual particles in aggregates. Numbers for apparently intact particles (that is, regular size and hexon negative) were determined in grey-scale mode by subtracting the number of hexon-positive particles (green channel) from the number of total particles. This was carried out inverting the hexon image of a given optical section, multiplying with the corresponding Ad2–TR image and recounting of the remaining regular particles. Stack projections were generated in NIH image (brightest point) and pseudo-coloured with Adobe Photoshop. FISH assays of Ad2 and Ad3 DNA were performed as described previously[3].

Sequence alignments

Ad2-hexon sequences were aligned using the pileup command (GapWeight = 3.0, GapLengthWeight = 0.10) of the Wisconsin Package software, version 10.0 from the Genetics Computer Group (GCG, Madison).

RECEIVED 1 MAY 2001; REVISED 7 AUGUST 2001; ACCEPTED 19 SEPTEMBER 2001; PUBLISHED 2 NOVEMBER 2001.

1. Whittaker, G. R., Kann, M. & Helenius, A. Viral entry into the nucleus. *Annu. Rev. Cell Dev. Biol.* **16,** 627–651 (2000).
2. Shenk, T. in *Fundamental Virology* (eds Fields, B. N., Knipe, D. M. & Howley, P. M.) 979–1016 (Lippincott-Raven, New York, 1996).
3. Greber, U. F. *et al.* The role of the nuclear pore complex in adenovirus DNA entry. *EMBO J.* **16,** 5998–6007 (1997).
4. Nakano, M. Y., Boucke, K., Suomalainen, M., Stidwill, R. P. & Greber, U. F. The first step of adenovirus type 2 disassembly occurs at the cell surface, independently of endocytosis and escape to the cytosol. *J. Virol.* **74,** 7085–7095 (2000).
5. Greber, U. F., Willetts, M., Webster, P. & Helenius, A. Stepwise dismantling of adenovirus 2 during entry into cells. *Cell* **75,** 477–486 (1993).
6. Stoffler, D., Fahrenkrog, B. & Aebi, U. The nuclear pore complex: from molecular architecture to functional dynamics. *Curr. Opin. Cell Biol.* **11,** 391–401 (1999).
7. Rout, M. P. *et al.* The yeast nuclear pore complex: composition, architecture, and transport mechanism. *J. Cell Biol.* **148,** 635–651 (2000).
8. Ryan, K. J. & Wente, S. R. The nuclear pore complex: a protein machine bridging the nucleus and cytoplasm. *Curr. Opin. Cell Biol.* **12,** 361–371 (2000).
9. Gorlich, D. & Kutay, U. Transport between the cell nucleus and the cytoplasm. *Annu. Rev. Cell Dev. Biol.* **15,** 607–660 (1999).
10. Rexach, M. & Blobel, G. Protein import into nuclei: association and dissociation reactions involving transport substrate, transport factors, and nucleoporins. *Cell* **83,** 683–692 (1995).
11. Snow, C. M., Senior, A. & Gerace, L. Monoclonal antibodies identify a group of nuclear pore complex glycoproteins. *J. Cell Biol.* **104,** 1143–1156 (1987).
12. Wisnivesky, J. P., Leopold, P. L. & Crystal, R. G. Specific binding of the adenovirus capsid to the nuclear envelope. *Hum. Gene Ther.* **10,** 2187–2195 (1999).
13. Panté, N., Bastos, R., McMorrow, I., Burke, B. & Aebi, U. Interactions and three-dimensional localization of a group of nuclear pore complex proteins. *J. Cell Biol.* **126,** 603–617 (1994).
14. Fornerod, M., Boer, J., van Baal, S., Morreau, H. & Grosveld, G. Interaction of cellular proteins with the leukemia specific fusion proteins DEK-CAN and SET-CAN and their normal counterpart, the nucleoporin CAN. *Oncogene* **13,** 1801–1808 (1996).
15. Chi, N. C., Adam, E. J. H. & Adam, S. A. Sequence and characterization of cytoplasmic nuclear protein import factor p97. *J. Cell Biol.* **130,** 265–274 (1995).
16. Yokoyama, N. *et al.* A giant nucleopore protein that binds Ran/TC4. *Nature* **376,** 184–188 (1995).
17. Greber, U. F. & Gerace, L. Nuclear protein import is inhibited by an antibody to a lumenal epitope of a nuclear pore complex glycoprotein. *J. Cell Biol.* **116,** 15–30 (1992).
18. Nakielny, S., Shaikh, S., Burke, B. & Dreyfuss, G. Nup153 is an M9-containing mobile nucleoporin with a novel ran-binding domain. *EMBO J.* **18,** 1982–1995 (1999).
19. Nakano, M. Y. & Greber, U. F. Quantitative microscopy of fluorescent adenovirus entry. *J. Struct. Biol.* **129,** 57–68 (2000).
20. Greber, U. F., Webster, P., Weber, J. & Helenius, A. The role of the adenovirus protease in virus entry into cells. *EMBO J.* **15,** 1766–1777 (1996).
21. Cerf, C. *et al.* Homo- and heteronuclear two-dimensional NMR studies of the globular domain of histone H1: full assignment, tertiary structure, and comparison with the globular domain of histone H5. *Biochemistry* **33,** 11079–11086 (1994).
22. Thomas, J. O. Histone H1: location and role. *Curr. Opin. Cell Biol.* **11,** 312–317 (1999).
23. Rux, J. J. & Burnett, R. M. Type-specific epitope locations revealed by X-ray crystallographic study of adenovirus type 5 hexon. *Mol. Ther.* **1,** 18–30 (2000).
24. Bustin, M. Preparation and application of immunological probes for nucleosomes. *Methods Enzymol.* **170,** 214–51 (1989).
25. Jakel, S. *et al.* The importin beta/importin 7 heterodimer is a functional nuclear import receptor for histone H1. *EMBO J.* **18,** 2411–2423 (1999).
26. Sodeik, B. Mechanisms of viral transport in the cytoplasm. *Trends Microbiol.* **8,** 465–472 (2000).
27. Suomalainen, M., Nakano, M. Y., Boucke, K., Keller, S. & Greber, U. F. Adenovirus-activated PKA and p38/MAPK pathways boost microtubule-mediated nuclear targeting of virus. *EMBO J.* **20,** 1310–1319 (2001).
28. Ojala, P. M., Sodeik, B., Ebersold, M. W., Kutay, U. & Helenius, A. Herpes simplex virus type 1 entry into host cells: reconstitution of capsid binding and uncoating at the nuclear pore complex in vitro. *Mol. Cell. Biol.* **20,** 4922–4931 (2000).
29. Russell, W. C. Update on adenovirus and its vectors. *J. Gen. Virol.* **81,** 2573–2604 (2000).
30. Fornerod, M. *et al.* The human homologue of yeast CRM1 is in a dynamic subcomplex with CAN/Nup214 and a novel nuclear pore component Nup88. *EMBO J.* **16,** 807–816 (1997).
31. Huber, J. *et al.* Snurportin1, an m3G-cap-specific nuclear import receptor with a novel domain structure. *EMBO J.* **17,** 4114–4126 (1998).
32. Doenecke, D. *et al.* Histones: genetic diversity and tissue-specific gene expression. *Histochem. Cell Biol.* **107,** 1–10 (1997).
33. Parseghian, M. H., Henschen, A. H., Krieglstein, K. G. & Hamkalo, B. A. A proposal for a coherent mammalian histone H1 nomenclature correlated with amino acid sequences. *Protein Sci.* **3,** 575–587 (1994).
34. Leclerc, D., Chapdelaine, Y. & Hohn, T. Nuclear targeting of the cauliflower mosaic virus coat protein. *J. Virol.* **73,** 553–560 (1999).
35. Kann, M., Sodeik, B., Vlachou, A., Gerlich, W. H. & Helenius, A. Phosphorylation-dependent binding of hepatitis B virus core particles to the nuclear pore complex. *J. Cell Biol.* **145,** 45–55 (1999).
36. Mabit, H., Breiner, K. M., Knaust, A., Zachmann-Brand, B. & Schaller, H. Signals for bidirectional nucleocytoplasmic transport in the duck hepatitis B virus capsid protein. *J. Virol.* **75,** 1968–1977 (2001).
37. Lever, M. A., Th'ng, J. P., Sun, X. & Hendzel, M. J. Rapid exchange of histone H1.1 on chromatin in living human cells. *Nature* **408,** 873–876 (2000).
38. Misteli, T., Gunjan, A., Hock, R., Bustin, M. & Brown, D. T. Dynamic binding of histone H1 to chromatin in living cells. *Nature* **408,** 877–881 (2000).
39. Saphire, A. C. S., Guan, T. L., Schirmer, E. C., Nemerow, G. R. & Gerace, L. Nuclear import of adenovirus DNA in vitro involves the nuclear protein import pathway and hsc70. J. Biol. Chem. **275,** 4298–4304 (2000).
40. Suomalainen, M. *et al.* Microtubule-dependent minus and plus end-directed motilities are competing processes for nuclear targeting of adenovirus. *J. Cell Biol.* **144,** 657–672 (1999).
41. Pinol-Roma, S. & Dreyfuss, G. Shuttling of pre-mRNA binding proteins between nucleus and cytoplasm. *Nature* **355,** 730–732 (1992).
42. Yokoyama, N. *et al.* A giant nucleopore protein that binds Ran/TC4. *Nature* **376,** 184–188 (1995).
43. Bustin, M. & Stollar, B. D. Immunochemical specificity in lysine-rich histone subfractions. *J. Biol. Chem.* **247,** 5716–21 (1972).
44. Melchior, F., Paschal, B., Evans, J. & Gerace, L. Inhibition of nuclear protein import by nonhydrolyzable analogues of GTP and identification of the small GTPase Ran/TC4 as an essential transport factor. *J. Cell Biol.* **123,** 1649–1659 (1993).
45. Drabent, B., Kunz, C. & Doenecke, D. A rat histone H2B pseudogene is closely associated with the histone H1d gene. *Biochim. Biophys. Acta* **1172,** 193–196 (1993).

ACKNOWLEDGEMENTS

We thank P. Groscurth for access to the confocal laser scanning microscope and P. Sonderegger for access to the SMART system, U. Ziegler and P. Cinelli for assistance and U. Aebi, U. Kutay and T. Misteli for comments on the manuscript. Numerous investigators are gratefully acknowledged for their gifts of reagents (and are indicated in the Methods section) and H. van der Velde is acknowledged for preparation of C terminus CAN/Nup214. The work was supported by the Swiss National Science Foundation and the Kanton of Zürich. Supplementary Information is available on *Nature Cell Biology*'s website (http://cellbio.nature.com).

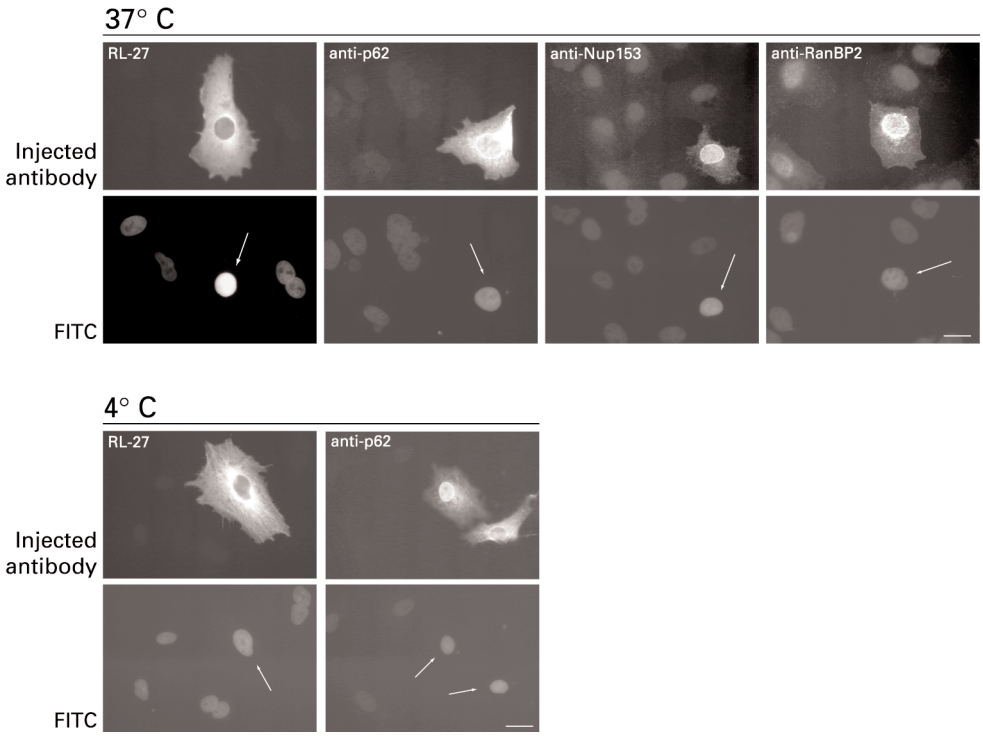

Supplementary Figure S1. **Microinjected anti-NPC antibodies reduce nuclear import of FITC–BSA–NLS.** A549 cells were microinjected at 4 °C with a mixture of FITC–BSA–NLS (0.5 mg ml^{-1}) and the indicated antibodies (0.5 mg ml^{-1}). After incubation at 4 °C for 45 min cells were either fixed with para-formaldehyde or transferred to 37 °C for 20 min and then fixed. Injected antibodies were visualised with Alexa 594-conjugated secondary antibodies and images recorded by fluorescence microscopy as described previously[3]. Note that all the cell nuclei are visible due to background autofluorescence. Cells that received FITC–BSA–NLS are pointed out by arrows. Scale bars, 20 μm.

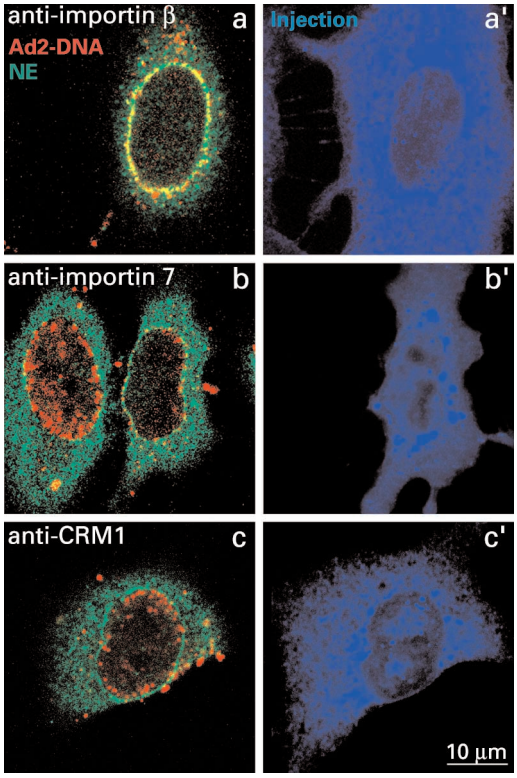

Supplementary Figure S2 **Histone H1 import factors are required for nuclear import of Ad2-DNA.** A549 cells were microinjected with the indicated antibodies, infected with Ad2 (3 μg per assay) and analysed by CLSM as described in Fig. 7B.